Structural characterization of a subtype-selective ligand reveals a novel mode of estrogen receptor antagonism

Andrew K. Shiau[1,2], Danielle Barstad[3], James T. Radek[3], Marvin J. Meyers[4], Kendall W. Nettles[3], Benita S. Katzenellenbogen[5], John A. Katzenellenbogen[4], David A. Agard[1] and Geoffrey L. Greene[3]

[1]The Howard Hughes Medical Institute and Department of Biochemistry and Biophysics, University of California, San Francisco, California 94143, USA. [2]Tularik Inc., Two Corporate Drive, South San Francisco, California 94080, USA. [3]The Ben May Institute for Cancer Research and Department of Biochemistry and Molecular Biology, University of Chicago, Chicago, Illinois 60637, USA. [4]Department of Chemistry, University of Illinois, Urbana, Illinois 61801, USA. [5]Departments of Molecular and Integrative Physiology and Cell and Structural Biology, University of Illinois, Urbana, Illinois 61801, USA

Published online: 15 April 2002, DOI: 10.1038/nsb787

The *R,R* enantiomer of 5,11-*cis*-diethyl-5,6,11,12-tetrahydrochrysene-2,8-diol (THC) exerts opposite effects on the transcriptional activity of the two estrogen receptor (ER) subtypes, ERα and ERβ. THC acts as an ERα agonist and as an ERβ antagonist. We have determined the crystal structures of the ERα ligand binding domain (LBD) bound to both THC and a fragment of the transcriptional coactivator GRIP1, and the ERβ LBD bound to THC. THC stabilizes a conformation of the ERα LBD that permits coactivator association and a conformation of the ERβ LBD that prevents coactivator association. A comparison of the two structures, taken together with functional data, reveals that THC does not act on ERβ through the same mechanisms used by other known ER antagonists. Instead, THC antagonizes ERβ through a novel mechanism we term 'passive antagonism'.

The physiological effects of both endogenous and synthetic estrogens are mediated by the estrogen receptors (ERs), ERα and ERβ, which are members of the nuclear receptor (NR) superfamily of ligand-regulated transcription factors[1,2]. In a search for ER subtype-selective ligands, the *R,R* enantiomer of 5,11-*cis*-diethyl-5,6,11,12-tetrahydrochrysene-2,8-diol (THC) (Fig. 1*a*) was determined to be a novel ER ligand, with an approximate six-fold affinity preference for ERβ over ERα and profoundly different activation profiles on the two ERs[3,4]. THC functions as an agonist on ERα, with an EC_{50} of ~3 nM, but has no effect on the transcriptional activity of ERβ. Instead, this compound potently antagonizes the effects of the endogenous estrogen 17β-estradiol (E2) on ERβ, with an IC_{50} < 10 nM. Consistent with these subtype-specific effects on transcriptional activation, THC also affects the two ERs differently in protease protection and other biochemical assays[5].

The C-terminal ligand-binding domains (LBDs) of ERα and ERβ each contain a ligand-responsive transcriptional activation function (AF-2)[6–9]. Agonists, such as E2 and diethylstilbestrol (DES), increase AF-2 activity. In contrast, pure antagonists, such as ICI 164,384 (ICI), and mixed-function partial agonist/antagonists, such as 4-hydroxytamoxifen (OHT) and raloxifene (RAL), block AF-2 activity[10–12] (Fig. 1*a*). The effects of THC on the transcriptional activity of fusions between the GAL4 DNA-binding domain and the two ER LBDs indicate that THC stimulates ERα AF-2 activity and inhibits agonist-induced ERβ AF-2 activity (data not shown), consistent with its effects on the full-length receptors.

Structural studies indicate that NR ligands regulate AF-2 activity by modulating the structure of NR LBDs[13,14]. NR ligands bind to their cognate receptors within a hydrophobic pocket formed within the core of the narrower or 'lower' half of the LBD. The binding of an agonist to an NR LBD stabilizes the positioning of the most C-terminal helix of the LBD, helix 12, such that it lies across the opening to the binding pocket formed by

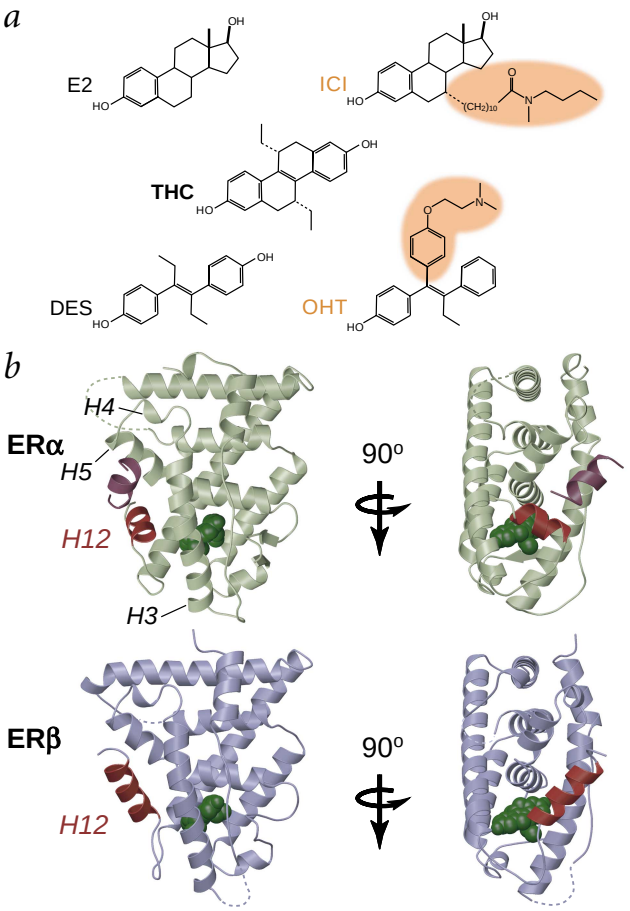

Fig. 1 Overall structures of the THC–ER LBD complexes. ***a***, Chemical structures of 17β-estradiol (E2), ICI 164,384 (ICI), diethylstilbestrol (DES), 4-hydroxytamoxifen (OHT) and *R,R*-5,11-*cis*-diethyl-5,6,11,12-tetrahydrochrysene-2,8-diol (THC). The side chains of ICI and OHT are highlighted in orange. ***b***, Two equivalent orthogonal views of the THC–ERα LBD–GRIP1 NR box II peptide and the THC–ERβ LBD complexes, showing that the two ER LBDs adopt distinct conformations when bound to THC. Both the ERα and ERβ LBDs are depicted in ribbon representation and colored light green and blue, respectively. In both complexes, helix 12 is colored red, and THC (green) is shown in space-filling representation. In the ERα complex, the coactivator peptide is depicted as a purple ribbon, and helices 3, 4, 5 and 12 have been labeled H3, H4, H5, and H12. Dashed lines represent regions of the structures that have not been modeled. Panel (*b*) and Figs 2*a*, 3*a*,*c* and 4 were generated using BOBSCRIPT[32] and rendered using Raster3D[33].

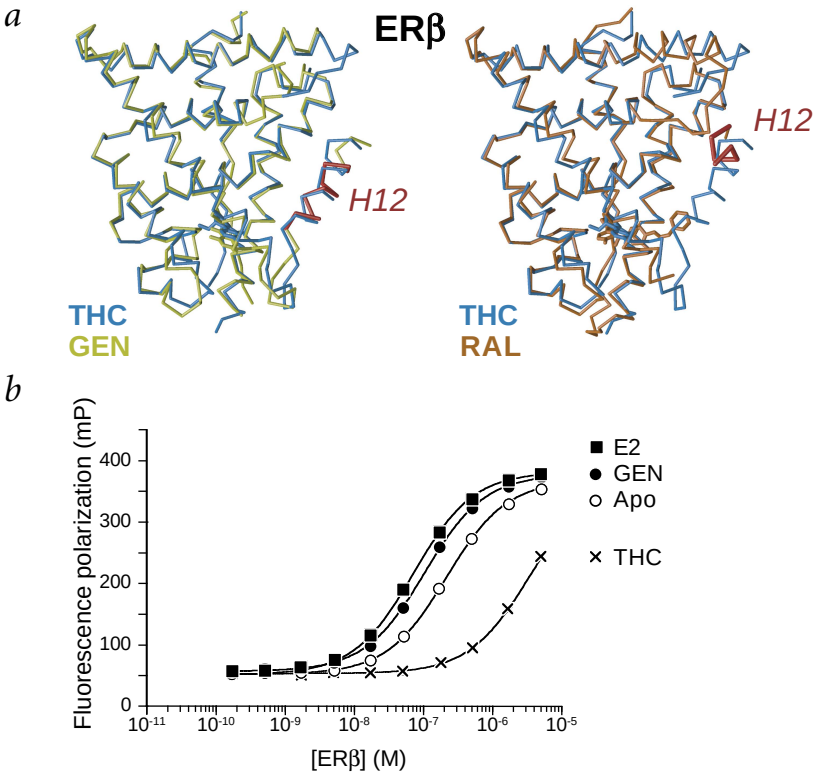

Fig. 2 Conformational equilibrium of helix 12. ***a***, Superpositions of the Cα trace of the THC–ERβ LBD complex (light blue) on those of the GEN–ERβ LBD (yellow) and the RAL–ERβ LBD (orange) complexes. Helix 12 in the RAL and GEN structures is colored red. Least squares superpositions were generated using LSQMAN[34] (THC/RAL has 1.0 Å r.m.s. deviation over 196 matched atoms with a 3.8 Å cutoff, and THC/GEN has 1.1 Å r.m.s. deviation over 218 matched atoms with a 3.8 Å cutoff). Helix 12 from each of the monomers in the THC–ERβ, GEN–ERβ and THC–ERα crystals is located in a distinct packing environment, indicating that the similarities/differences in helix 12 positioning among these complexes are not the consequence of crystal lattice effects. ***b***, Equilibrium binding of a rhodamine-labeled Leu-X-X-Leu-Leu motif-containing peptide to the ERβ LBD alone or bound to E2, DES, GEN and THC was analyzed by measuring fluorescence polarization as a function of receptor or ligand–receptor complex concentration. Values represent the mean ± s.d. for each experimental condition performed in triplicate, and the data were fit using nonlinear least squares analysis (K_d[E2] = 71 ± 2 nM, K_d[GEN] = 104 ± 4 nM, K_d[apo] = 215 ± 5 nM and K_d[THC] = 3.3 ± 0.3 μM).

helices 3, 5/6 and 11. This conformation of the LBD allows the receptor to interact with a class of proteins known as transcriptional coactivators, which mediate ligand-dependent transcription of NRs[15]. p160 coactivators recognize agonist-bound NR LBDs *via* the short sequence motif, Leu-X-X-Leu-Leu (where X is any amino acid), called the NR box[15]. NR boxes form amphipathic α-helices that recognize a hydrophobic groove on the surface of an agonist-bound LBD formed by residues from helices 3, 4, 5 and 12 (ref. 13). NR AF-2 antagonists sterically preclude the proper formation of the NR box-binding site[13,14]. The structures of the BMS614–retinoic acid receptor-α[16], OHT–ERα[17], RAL–ERα[18], RAL–ERβ[19] and ICI–ERβ[20] LBD complexes reveal that each of these antagonists possesses a bulky side chain (Fig. 1*a*) that cannot be contained within the ligand binding pocket. These side chains protrude out of the opening to the binding pocket formed by helices 3, 5/6 and 11, thereby preventing helix 12 from adopting the agonist-bound conformation. The positioning of the side chains of BMS614, OHT and RAL forces helix 12 to adopt an alternative conformation in which it binds to and occludes the remainder of the coactivator binding site by mimicking the interactions formed by the NR box[16–19]. The ICI side chain, in contrast, binds directly to the coactivator-binding site of ERβ, causing helix 12 to be completely disordered[20]. The structure of the ERβ LBD bound to the ERβ partial agonist genistein (GEN) reveals that ligand binding can stabilize yet another conformation of helix 12 (ref. 19). In this complex, helix 12 is bound over the ligand-binding pocket in a position such that it occludes the coactivator recognition surface only partially. However, the functional significance of this conformation of the LBD is unclear.

Given its behavior in transactivation and other assays[3–5], THC would be predicted to both stabilize a conformation of the ERα LBD that favors coactivator binding and one of the ERβ LBD that precludes coactivator binding. However, because it lacks a bulky side chain similar to those of OHT, RAL and ICI, THC must antagonize ERβ through a fundamentally different mechanism (Fig. 1*a*). Here we describe structural and additional functional characterization of the effects of THC on ERα and ERβ. These studies indicate that THC exerts its effects on the AF-2 activity of the two ERs by stabilizing distinct conformations of the two receptors and that THC antagonizes ERβ through a novel mechanism we term 'passive antagonism'.

Structures of the THC–ER LBD complexes

Crystals of ERα LBD bound to both THC and a peptide containing the second NR box of the p160 coactivator GRIP1 (ref. 15), and the ERβ LBD bound to THC were grown. Both structures were determined by molecular replacement. The ERα complex structure has been refined to an R-factor of 20.3% (R_{free} = 24.3%) using data to 1.95 Å, and the ERβ complex structure has been refined to an R-factor of 25.9% (R_{free} = 29.9%) using data to 2.95 Å (Table 1; Figs 1*b*, 3*a*).

As anticipated, the ERα LBD when bound to THC adopts the same conformation as it does when bound to the full agonists E2 and DES[17,18] (Fig. 1*b*). Helix 12 adopts the agonist-bound conformation, which promotes NR box association. In contrast, the binding of THC to ERβ LBD does not stabilize the agonist-bound conformation of helix 12 (Fig. 1*b*). Surprisingly, helix 12 does not bind to the region of the coactivator recognition groove formed by helices 3, 4 and 5 as it does in the OHT–ERα, RAL–ERα and RAL–ERβ complexes, and it is not disordered as it is in the ICI–ERβ complex (Fig. 2*a*). Instead, helix 12 in the THC–ERβ complex adopts an orientation most similar to that observed in the GEN–ERβ complex (Fig. 2*a*). In both complexes, helix 12 is stabilized in this conformation by hydrophobic contacts formed by Val 487, Leu 491, Met 494 and Leu 495 with the rest of the LBD[19] (data not shown).

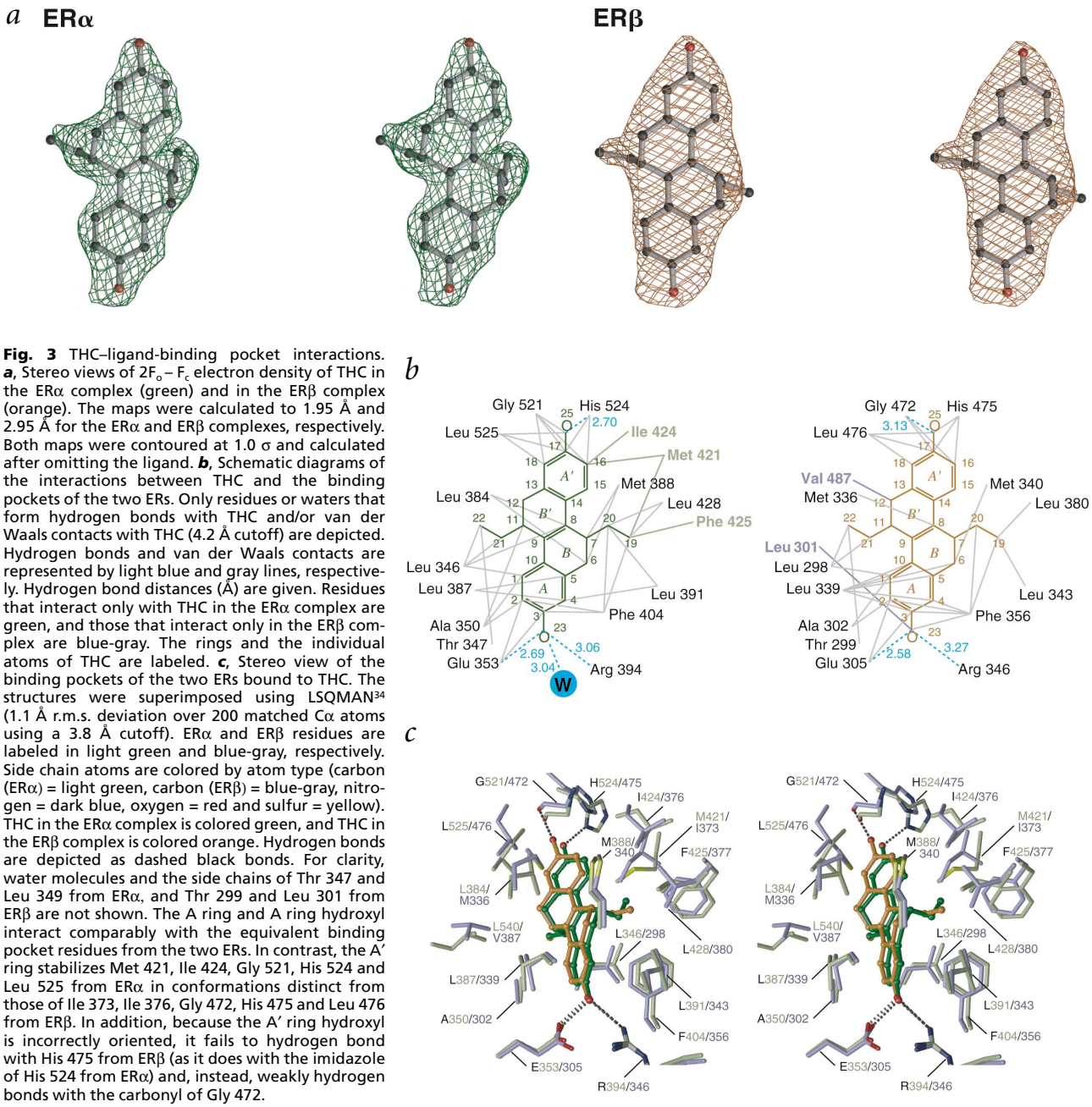

Fig. 3 THC–ligand-binding pocket interactions. ***a***, Stereo views of $2F_o - F_c$ electron density of THC in the ERα complex (green) and in the ERβ complex (orange). The maps were calculated to 1.95 Å and 2.95 Å for the ERα and ERβ complexes, respectively. Both maps were contoured at 1.0 σ and calculated after omitting the ligand. ***b***, Schematic diagrams of the interactions between THC and the binding pockets of the two ERs. Only residues or waters that form hydrogen bonds with THC and/or van der Waals contacts with THC (4.2 Å cutoff) are depicted. Hydrogen bonds and van der Waals contacts are represented by light blue and gray lines, respectively. Hydrogen bond distances (Å) are given. Residues that interact only with THC in the ERα complex are green, and those that interact only in the ERβ complex are blue-gray. The rings and the individual atoms of THC are labeled. ***c***, Stereo view of the binding pockets of the two ERs bound to THC. The structures were superimposed using LSQMAN[34] (1.1 Å r.m.s. deviation over 200 matched Cα atoms using a 3.8 Å cutoff). ERα and ERβ residues are labeled in light green and blue-gray, respectively. Side chain atoms are colored by atom type (carbon (ERα) = light green, carbon (ERβ) = blue-gray, nitrogen = dark blue, oxygen = red and sulfur = yellow). THC in the ERα complex is colored green, and THC in the ERβ complex is colored orange. Hydrogen bonds are depicted as dashed black bonds. For clarity, water molecules and the side chains of Thr 347 and Leu 349 from ERα, and Thr 299 and Leu 301 from ERβ are not shown. The A ring and A ring hydroxyl interact comparably with the equivalent binding pocket residues from the two ERs. In contrast, the A′ ring stabilizes Met 421, Ile 424, Gly 521, His 524 and Leu 525 from ERα in conformations distinct from those of Ile 373, Ile 376, Gly 472, His 475 and Leu 476 from ERβ. In addition, because the A′ ring hydroxyl is incorrectly oriented, it fails to hydrogen bond with His 475 from ERβ (as it does with the imidazole of His 524 from ERα) and, instead, weakly hydrogen bonds with the carbonyl of Gly 472.

Ligands and helix 12 positioning

Based on the position of helix 12, the ERβ LBD in the conformation stabilized by THC and GEN should be incapable of interacting with coactivators and, hence, transcriptionally silent[19]. However, GEN and THC clearly show different activities on ERβ in mammalian cells: GEN is a partial agonist[9] and THC is a pure antagonist[3,4]. How can the structural data be reconciled with the different activities of these compounds in transcriptional assays?

The simplest model that explains these data is based on two hypotheses. First, helix 12 in the unliganded ERβ LBD is in equilibrium between the inactive conformation observed in the THC– and GEN–ERβ LBD structures and the active agonist-bound conformation. Second, rather than inducing a single static conformation of helix 12, ligands affect LBD transcriptional activity by shifting this equilibrium. As a consequence, helix 12 in the unliganded or apo ERβ LBD, although largely in a transcriptionally silent conformation, may also adopt a transcriptionally active one. Hence, the low but detectable constitutive AF-2-derived transcriptional activity of the unliganded receptor[9] results from the modest but significant ability of the apo LBD to bind coactivator. Full agonists, such as E2 and DES, shift the helix 12 conformational equilibrium in favor of the active conformation and stimulate AF-2 activity by increasing the affinity of the LBD for coactivator. Because partial agonists, such as GEN, are incapable of shifting the equilibrium in favor of the active conformation to the same extent as full agonists, they are able only to incrementally increase the affinity of the receptor for coactivator and, hence, activate AF-2 less efficiently than full

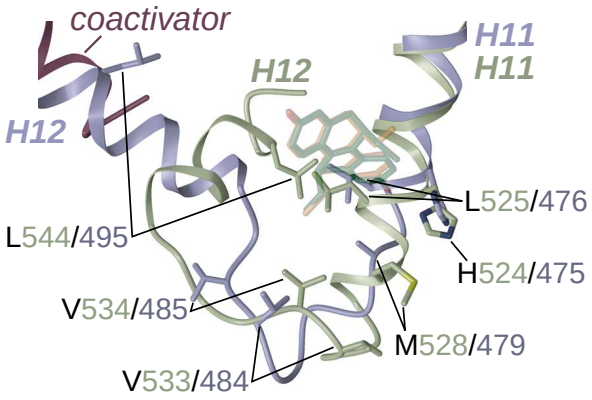

Fig. 4 Ligand-binding pocket residues influence helix 12 positioning. The structures of the two complexes were superimposed, and the side chains and ligands are colored as in Fig. 3*c*. In addition, the peptide backbone of ERα, ERβ and the coactivator peptide are colored light green, blue-gray and purple, respectively. In each structure, helices 11 and 12 are labeled H11 and H12, and, for clarity, the ligands have been made semi-transparent. The side chain of Met 479 from ERβ is disordered and depicted as an Ala residue. In the ERα complex, His 524, Leu 525 and Met 528 are oriented by the THC A′ ring such that they can form nonpolar contacts with residues from helix 12 or the preceding loop (Val 533, Val 534 and Leu 544). Because of the distinct positioning of His 475 and Leu 476 (His 524 and Leu 525 in ERα) stabilized by the A′ ring, the equivalent interactions do not occur in the ERβ complex.

agonists. GEN binding should permit the ERβ LBD to sample both inactive and active conformations of helix 12 (possibly to comparable extents). The observation of the inactive conformation in the GEN complex structure may reflect the true bias of the equilibrium in solution or it may result from the influence of the crystallization conditions on the equilibrium.

In principle, THC could antagonize receptor activity by shifting the equilibrium to favor the inactive THC/GEN-bound conformation. If THC binding forces the receptor to sample this conformation more than it does in the absence of ligand, the THC–receptor complex would be expected to have an even lower affinity for coactivator than the unliganded receptor. This would agree with the absence of transcriptional activity of the THC–ERβ complex and the conformation of helix 12 observed in the crystal.

The helix 12 conformational equilibrium would be difficult to observe directly. Nonetheless, the predicted actions of the various ligands, inferred from the model described above, suggest a testable hypothesis. The binding of different ligands should modulate the affinity of the ERβ LBD for coactivator such that E2–LBD > GEN–LBD > apo LBD > THC–LBD. The affinities of various ligand–ERβ LBD complexes for an Leu-X-X-Leu-Leu motif-containing peptide were directly measured using a fluorescence polarization-based binding assay[21], and the expected rank order of affinities was observed for the different complexes (Fig. 2*b*). Thus, these and other biochemical data[5] suggest that helix 12 positioning in ERβ, as in the case of other NRs[13], is dictated by a ligand-sensitive conformational equilibrium.

THC–ligand binding pocket interactions

When ER agonists bind to ERα (and presumably ERβ), they favor the active conformation of helix 12 but they do so indirectly. These ligands form hydrogen bonds and van der Waals contacts with residues from helices 3, 6, 8 and 11 and the β-hairpin, positioning these residues in conformations that allow their interaction with each other and with neighboring residues surrounding the binding pocket. The formation of these cooperative interactions positions residues from helices 3, 5 and 11 such that they create a predominantly hydrophobic binding surface for the loop connecting helices 11 and 12 and helix 12 itself[17,18].

THC interacts with the ERα LBD similar to the full agonists, DES and E2, and nucleates all of the polar and nonpolar interactions required to favor the positioning of helix 12 in the agonist-bound conformation[17,18] (Fig. 3*b*,*c*). For example, in the ERα complex, the A′ ring forms hydrogen bonds and/or nonpolar contacts with the side chains of His 524 and Leu 525 (Fig. 3*b*,*c*), stabilizing them in conformations such that they form (either directly or indirectly) part of the binding site for helix 12 or the preceding loop. The side chain of His 524 forms hydrophobic contacts with the side chain of Met 528, positioning it such that it can, in turn, form nonpolar contacts with the side chains of Val 533 and Val 534 from the loop between helices 11 and 12 (Fig. 4). The side chain of Leu 525 packs against that of Leu 544 from helix 12 (Fig. 4).

Although it binds to ERβ in a similar overall manner, THC fails to stabilize many of the interactions in the A′ ring region of the binding pocket that were observed in the ERα complex (Fig. 3*b*,*c*). In the ERβ complex, the B-ring ethyl group adopts a more extended conformation than in the ERα complex, causing the tetrahydrochrysene scaffold to be tilted by 5° towards the opening formed by helices 3, 5 6 and 11, and away from the floor of the binding pocket. Because the A′ ring is displaced by ~0.7 Å from its position in the ERα complex (Fig. 3*c*), the side chains of His 475 and Leu 476 (which form only nonpolar contacts with the A′ ring) are positioned ~1.6 and 2.3 Å away, respectively, from the locations of their counterparts in the ERα complex (His 524 and Leu 525) (Figs 3*c*, 4). As a result, the side chain of His 475 fails to pack against that of Met 479 (equivalent to Met 528 in ERα), causing the Met 479 side chain to be disordered. The backbone atoms of Met 479 and the residues flanking it adopt a random coil conformation (as compared to the helical conformation adopted by their counterparts in ERα), and Met 479 is located 2.4 Å distant from Met 528 (based on Cα atoms) (Fig. 4). Consequently, both Leu 476 and Met 479 are not positioned appropriately to form interactions with relevant residues from helix 12 and the preceding loop (Val 484, Val 485 and Leu 495) that would stabilize the active conformation of helix 12 (Fig. 4). Therefore, these residues destabilize the active conformation of helix 12 (Fig. 4). Thus, by positioning certain binding pocket residues in nonproductive conformations, the binding of THC to ERβ disfavors the agonist-bound conformation of helix 12 and shifts the equilibrium towards the inactive conformation of helix 12.

The two ligand-binding pocket residues that differ between the two subtypes may explain the failure of THC to act as an ERβ agonist. Met 336 and Ile 373 in ERβ (equivalent to Leu 384 and Met 421 in ERα) are positioned on opposite faces of THC (Fig. 3*b*,*c*). Modeling (based on both the THC–ERα and GEN–ERβ structures) suggests that the THC A′ ring would have to be positioned ~2.4 Å lower in the ERβ binding pocket relative to its location in the crystal in order for THC to both interact with Met 336 and Ile 373 and orient His 475 and Leu 476 in productive conformations (data not shown). This lower position should be highly unfavorable because it would result in steric clashes between the B′ ring ethyl group and the side chain of

Table 1 Summary of Crystallographic Statistics

Data collection		
Complex	THC–ERα LBD–GRIP1 NR Box II peptide	THC–ERβ LBD
Space group	$P2_1$	R3
Resolution (Å)[1]	1.95 (2.02–1.95)	2.95 (3.06–2.95)
Observations		
Total	119,409	64,540
Unique	34,533	14,895
Completeness (%)[1]	97.9 (97.7)	99.7 (100)
R_{sym} (%)[1,2]	6.5 (53.1)	4.5 (30.2)
$\langle I \rangle / \langle \sigma (I) \rangle$[1]	18.8 (2.9)	23.3 (3.4)
Refinement		
Number of atoms		
Protein	3,830	3,409
Water	166	9
Heterogen	53	48
R_{cryst} (%)[1,3]	20.3 (29.6)	25.9 (34.0)
R_{free} (%)[1,3]	24.3 (33.6)	29.9 (35.1)
R.m.s. deviation		
Bonds (Å)	0.005	0.011
Angles (°)	1.08	1.29
Average B-factor (Å²)	38.5	40.1

[1]Values in parentheses refer to the highest resolution shell.
[2]$R_{sym} = \Sigma|I_h - \langle I_h \rangle| / \Sigma I_h$, where I_h is the integrated intensity of a given reflection and $\langle I_h \rangle$ is the average intensity over symmetry equivalents.
[3]$R_{cryst} = \Sigma||F_o| - |F_c|| / \Sigma|F_o|$, where F_o and F_c are observed and calculated amplitudes, respectively. R_{free} is calculated similarly using a test set of reflections.

Leu 298 at floor of the binding pocket (Fig. 3*b*,*c*). THC presumably binds in the alternative mode observed in the crystal to avoid these steric clashes. Consistent with this, the dimethyl analog of THC, which should be less sterically hindered from adopting the lower position, acts as a weak ERβ partial agonist[3].

Antagonism without a side chain

Because the positioning of the side chains of OHT, RAL and ICI directly or 'actively' precludes the agonist-bound conformation of helix 12 by steric hindrance[13,14], we term their common mechanism of action as 'active antagonism'. Clearly, THC lacks a bulky side chain, and in its complex with ERβ, helix 12 is not sterically precluded from adopting the agonist-bound conformation (Fig. 4). Instead, THC antagonizes ERβ by stabilizing nonproductive conformations of key residues in the ligand-binding pocket, thereby disfavoring the equilibrium to the agonist-bound conformation of helix 12 and leading to stabilization of an inactive conformation of helix 12. Thus, we call the mechanism of antagonism of THC 'passive antagonism'.

Passive antagonism may not be unique to THC and ERβ. There are many examples of NR ligands that act as antagonists even though they are smaller than the endogenous agonists of these NRs. The synthetic androgen receptor antagonist, flutamide, is comparable in size to testosterone and does not possess an obvious moiety that would act as an antagonist side chain[22]. Similarly, progesterone is smaller than aldosterone but is a high affinity antagonist of the mineralocorticoid receptor[23].

Many NRs have several subtypes that possess distinct expression patterns and regulate distinct target genes[24]. Antagonists generated through the addition of bulky side chains to agonist scaffolds are limited to being antagonistic on one or more subtypes of a particular NR[13,14]. The passive antagonism mechanism, as revealed here through direct comparison of the two THC–ER LBD complexes, suggests a new approach to achieving NR antagonism. Compounds could be designed to selectively stabilize the inactive conformations of certain NR subtypes and the active conformations of others. Such ligands may exert novel biological and therapeutic effects.

Methods

Protein expression and purification. The human ERα LBD (residues 297–554) was expressed, carboxymethylated and purified as described[17]. For crystallographic studies, the human ERβ LBD (residues 256–505) was expressed as an N-terminally His_6-tagged fusion protein in BL21(DE3)pLysS cells using a modified pET-15b plasmid (Novagen). Bacterial lysates were applied to an estradiol-Sepharose column, and the bound ERβ LBD was carboxymethylated with 20 mM iodoacetic acid. Protein was eluted with 30 μM THC in ~50 ml of 20 mM Tris-HCl, 1 M urea and 10% (v/v) dimethyl formamide (DMF), pH 8.1. The ERβ LBD was further purified by ion exchange chromatography (Resource Q, Pharmacia). Protein samples were analyzed by SDS-PAGE, native PAGE and electrospray ionization mass spectrometry. For biochemical studies, residues 214–530 of human ERβ were expressed as a fusion with glutathione-S-transferase (GST) in BL21 cells using a modified pGEX-4T1 plasmid (Pharmacia). The GST fusion protein was bound to glutathione Sepharose 4 Fast Flow (Pharmacia) and eluted with glutathione per the manufacturer instructions. In some experiments, the protein was further purified by ion exchange chromatography (HiTrap Q, Pharmacia).

Crystallization and data collection. Crystals of the THC–ERα LBD–GRIP1 NR box II peptide complex were prepared by hanging drop vapor diffusion at 19–21 °C. Before crystallization, the THC–ERα LBD complex was incubated overnight with a four-fold molar excess of the GRIP1 NR box II peptide. Samples (0.5 μl) of this solution (5.0 mg ml^{-1} protein) were mixed with 3.5 μl of reservoir buffer consisting of 16% (w/v) PEG 4000, 53 mM Tris-HCl, pH 8.8, and 50 mM $MgCl_2$ and suspended over wells containing 800 μl of the reservoir buffer. The crystals lie in the spacegroup $P2_1$, with cell dimensions a = 54.55 Å, b = 82.60 Å, c = 59.04 Å and β = 111.53°. Two independent THC-LBD–peptide complexes form the asymmetric unit. A crystal was transferred to a cryo-solvent solution containing 20% (w/v) PEG 4000, 15% (v/v) ethylene glycol, 100 mM Tris-HCl, pH 8.6, and 100 mM $MgCl_2$ and frozen in an N_2 stream in a nylon loop. Diffraction data were measured at –170 °C at beamline 5.0.2 at the Advanced Light Source (ALS) using a Quantum 4 CCD camera (Area Detector Systems Corp.) at a wavelength of 1.10 Å. Images were processed with DENZO[25], and the integrated intensities were scaled with SCALEPACK[25] using the default –3 σ cutoff.

Crystals of the THC–ERβ LBD complex were obtained by hanging drop vapor diffusion at 21–23 °C. Samples (2 μl) of a solution of the complex (4.8 mg ml^{-1}) were combined with 2 μl samples of a reservoir solution containing 1.5–1.75 M $(NH_4)_2SO_4$ and 100 mM sodium acetate, pH 4.8–5.2, and suspended over wells containing 800 μl of reservoir solution. The resulting crystals belong to the space group R3, with cell parameters a = b = 99.14 Å and c = 193.38 Å (hexagonal setting). The asymmetric unit contains two ERβ LBD monomers that do not form the dimer observed in the ERα complex. Instead, each of the two LBDs interacts similarly with symmetry-related molecules to form crystallographic trimers. Before data collection, a single crystal was transferred to a stabilizing solution (1.8 M $(NH_4)_2SO_4$, 100 mM NaCl, 100 mM sodium acetate, pH 4.5, and 10 μM THC). The crystal was then sequentially transferred at 30 min intervals through a series of solutions consisting of the stabilizing solution supplemented with increasing concentrations of ethylene glycol (1% (v/v) increments) to a final concentration of 15% (v/v). The crystal was then flash frozen in an N_2 stream in a nylon loop. Diffraction data were measured at –170 °C at beamline 5.0.2 at the ALS using a Quantum 4 CCD camera at a wavelength of 1.07 Å. Images were processed with DENZO, and the integrated intensities were scaled with SCALEPACK using the default –3 σ cutoff.

Structure determination and refinement. The model of the DES–ERα LBD–GRIP1 NR box II peptide complex (3ERD) was modified by truncating the side chains of the ligand-binding pocket of both monomers to Ala and by removing all ligands, waters, carboxymethyl groups and ions. After subjecting this edited model to rigid body refinement in REFMAC[26], the missing parts of the model were built. The rest of the model was corrected using MOLOC[27] and two-fold averaged maps generated with DM[26]. All masks for averaging were generated using MAMA[28], and PHASES[29] and the CCP4 suite[26] were used for the generation of structure factors and the calculation of weights. Initially, positional refinement was performed using REFMAC. At later stages, the model was refined using the simulated annealing, positional and B-factor refinement protocols in CNS[30]. All B-factors were refined isotropically. Anisotropic scaling and a bulk solvent correction were used throughout refinement. The R_{free} set contains a random sample of 6.5% of all data. All data between 47 and 1.95 Å (with no σ cutoff) were used. The current model is composed of residues 305–459 and 469–547 of monomer A, residues 305–460 and 472–547 of monomer B, residues 687–696 of peptide A, residues 686–695 of peptide B, two ligand molecules, 166 water molecules, one carboxymethyl group and one chloride ion. According to PROCHECK[26], 96.6% of all residues in the model are in the core regions of the Ramachandran plot, and none are in the disallowed regions.

The intensities within the ERβ data set fall off very rapidly as a function of resolution (Wilson B-factor ~90 $Å^2$ calculated from 4.5 to 2.95 Å). To increase the contribution of the higher resolution terms, the data were sharpened with a correction factor of –55 $Å^2$. Maps calculated using this sharpened data revealed higher resolution features, such as improved side chain density[31]. All subsequent manipulations were performed using this sharpened data.

The two LBDs in the asymmetric unit were located by molecular replacement in AmoRe[26] and TFFC[26]. The search model was constructed by overlapping the models of five ERα LBD complexes (PDB entries 1A52, 1ERE, 1ERR, 3ERD and 3ERT) and setting the occupancies of each model to 20% (R-factor = 55.3% and correlation coefficient = 55.9% after placement of both monomers). The model was then built using MOLOC and two-fold averaged maps generated with DM. MAMA was used for all mask manipulations, and PHASES and the CCP4 suite were used for the generation of structure factors and the calculation of weights. Refinement was performed initially using the positional refinement protocols in REFMAC and, later, using the simulated annealing, positional and B-factor refinement protocols in CNS. All B-factors were refined isotropically. Anisotropic scaling, a bulk solvent correction, and tight noncrystallographic symmetry restraints were used throughout refinement. The R_{free} set contains a random sample of 5% of all data. All data between 49 and 2.95 Å (with no σ cutoff) were used. The current model is composed of residues 261–284, 290–408 and 413–501 of monomer A, the last residue of the affinity tag and residues 256– 280, 294–410, 413–479 and 485–497 of monomer B, two ligand molecules, and nine water molecules. According to PROCHECK[26], 92.5% of all residues in the model are in the core regions of the Ramachandran plot, and none are in the disallowed regions.

Peptide binding assay. Samples of the GST–ERβ LBD fusion protein, in the absence or presence of the various ligands (at saturating concentrations), were mixed with an Leu-X-X-Leu-Leu motif-containing peptide (Ile-Leu-Arg-Lys-Leu-Leu-Gln-Glu), which had been N-terminally labeled with rhodamine (reaction buffer = 10 mM HEPES-Na, 150 mM NaCl, 2 mM $MgCl_2$, 1 mM EDTA and 100 μg ml^{-1} BSA, pH 7.9, and [peptide] = 5 nM). The binding reactions were incubated at ambient temperature with shaking for 1 h in 96-well plates (Whatman), and the fluorescence polarization was measured on an Analyst reader (Molecular Devices). K_d values were generated from triplicate assays by nonlinear least squares analysis (Prism, GraphPad Software).

Coordinates. Coordinates of the structures have been deposited in the Protein Data Bank (accession codes 1L2I and 1L2J for the ERα and ERβ complexes, respectively).

Acknowledgments

We thank T. Earnest for advice and assistance at beamline 5.0.2 (ALS is funded by the US Department of Energy Office of Basic Energy Sciences). We also thank M. Butte, N. Ota and Y. Shibata for assistance with data collection; P. Coward, A. Derman, and Y. Li for comments on the manuscript; and H. Deacon for extensive graphical assistance. This work was supported by the NIH (B.S.K, J.A.K. and D.A.A), the Howard Hughes Medical Institute (D.A.A.), the Susan G. Komen Breast Cancer Foundation (G.L.G.), the USAMRMC (G.L.G.) and the Illinois Department of Public Health (G.L.G). In the initial phases of this work, A.K.S. was supported by a Howard Hughes Medical Institute Predoctoral Fellowship and a UCSF Chancellor's Fellowship. All crystallographic studies were completed while A.K.S. was at UCSF, and the peptide binding studies were performed by A.K.S. at Tularik Inc.

Competing interests statement

The authors declare competing financial interests: see the Nature Structural Biology website (*http://structbio.nature.com*) for details.

Correspondence should be addressed to A.K.S. *email: ashiau@tularik.com* or G.L.G. *email: ggreene@uchicago.edu*

Received 1 August, 2001; accepted 8 February, 2002.

1. Katzenellenbogen, B.S. & Katzenellenbogen, J.A. *Breast Cancer Res.* **2**, 335–344 (2000).
2. Pettersson, K. & Gustafsson, J.A. *Annu. Rev. Physiol.* **63**, 165–192 (2001).
3. Meyers, M.J., Sun, J., Carlson, K.E., Katzenellenbogen, B.S. & Katzenellenbogen, J.A. *J. Med. Chem.* **42**, 2456–2468 (1999).
4. Sun, J. *et al. Endocrinology* **140**, 800–804 (1999).
5. Kraichely, D.M., Sun, J., Katzenellenbogen, J.A. & Katzenellenbogen, B.S. *Endocrinology* **141**, 3534–3545 (2000).
6. Pham, T.A., Hwung, Y.P., Santiso-Mere, D., McDonnell, D.P. & O'Malley, B.W. *Mol. Endocrinol.* **6**, 1043–1050 (1992).
7. Tzukerman, M.T. *et al. Mol. Endocrinol.* **8**, 21–30 (1994).
8. McInerney, E.M., Weis, K.E., Sun, J., Mosselman, S. & Katzenellenbogen, B.S. *Endocrinology* **139**, 4513–4522 (1998).
9. Barkhem, T. *et al. Mol. Pharmacol.* **54**, 105–112 (1998).
10. Danielian, P.S., White, R., Lees, J.A. & Parker, M.G. *EMBO J.* **11**, 1025–1033 (1992).
11. Berry, M., Metzger, D. & Chambon, P. *EMBO J.* **9**, 2811–2818 (1990).
12. Kraus, W.L., McInerney, E.M. & Katzenellenbogen, B.S. *Proc. Natl. Acad. Sci. USA* **92**, 12314–12318 (1995).
13. Steinmetz, A.C., Renaud, J.P. & Moras, D. *Annu. Rev. Biophys. Biomol. Struct.* **30**, 329–359 (2001).
14. Weatherman, R.V., Fletterick, R.J. & Scanlan, T.S. *Annu. Rev. Biochem.* **68**, 559–581 (1999).
15. Glass, C.K. & Rosenfeld, M.G. *Genes Dev.* **14**, 121–141 (2000).
16. Bourguet, W. *et al. Mol. Cell* **5**, 289–298 (2000).
17. Shiau, A.K. *et al. Cell* **95**, 927–937 (1998).
18. Brzozowski, A. *et al. Nature* **389**, 753–758 (1997).
19. Pike, A.C. *et al. EMBO J.* **18**, 4608–4618 (1999).
20. Pike, A.C. *et al. Structure* **9**, 145–153 (2001).
21. Shiau, A.K., Coward, P., Schwarz, M. & Lehmann, J.M. *Curr. Opin. Drug Discov. Devel.* **4**, 575–590 (2001).
22. Singh, S.M., Gauthier, S. & Labrie, F. *Curr. Med. Chem.* **7**, 211–247 (2000).
23. Souque, A. *et al. Endocrinology* **136**, 5651–5658 (1995).
24. Mangelsdorf, D.J. *et al. Cell* **83**, 835–839 (1995).
25. Otwinowski, Z. & Minor, W. *Methods Enzymol.* **276**, 307–326 (1997).
26. Dodson, E.J., Winn, M. & Ralph, A. *Methods Enzymol.* **277**, 620–634 (1997).
27. Muller, K. *et al. Bull. Soc. Chim. Belge.* **97**, 655–667 (1988).
28. Kleywegt, G.J. & Jones, T.A. *Acta Crystallogr. D* **55**, 941–944. (1999).
29. Furey, W. & Swaminathan, S. *Methods Enzymol.* **277**, 590–619 (1997).
30. Brünger, A.T. *et al. Acta Crystallogr. D* **54**, 905–921 (1998).
31. Stehle, T., Gamblin, S.J., Yan, Y. & Harrison, S.C. *Structure* **4** 165–182 (1996).
32. Esnouf, R.M. *J. Mol. Graph. Model.* **15**, 132–134, 112–113 (1997).
33. Merritt, E.A. & Bacon, D.J. *Methods Enzymol.* **277**, 505–524 (1997).
34. Kleywegt, G.J. & Jones, T.A. *Methods Enzymol.* **277**, 525–545 (1997).